Monatshefte für Chemie 135, 1297–1304 (2004)
DOI 10.1007/s00706-004-0219-1

Monatshefte für Chemie
Chemical Monthly
Printed in Austria

Concerning the Photodiastereomerization and Protic Equilibria of Urocanic Acid and its Complex with Human Serum Albumin

Bettina Schwarzinger and **Heinz Falk***

Institute of Organic Chemistry, Johannes Kepler University Linz, A-4040 Linz, Austria

Received April 30, 2004; accepted May 4, 2004
Published online July 23, 2004

Summary. Photodiastereomerization of urocanic acid and its human serum albumin complex (its binding constant was estimated to amount $4.1 \cdot 10^{-4}\,dm^3 \cdot mol^{-1}$) was investigated. It was found that although the photodiastereomerization rates were similar, the photoequilibrium positions differed significantly ((*E*):(*Z*) = 33:77 for free urocanic acid, and 50:50 for the complex). This is thought to be due to a different stabilization of the corresponding orthogonal excited states. The thermal barrier of diastereomerization was estimated to amount to more than $250\,kJ \cdot mol^{-1}$ making it a very unlikely process under physiological and photodiastereomerization conditions. The various prototropic species of the two diastereomers at various *pH* values were analyzed by means of a mathematical model and from these results a novel photoinduced *pH*-jump methodology allowing for fast, persistent, diffusion controlled, and bidirectional jumps is proposed.

Keywords. Diastereomerization; Photochemistry; Protic equilibria; Thermal stability; *pH*-Jump.

Introduction

(*E*)-Urocanic acid (3-(1*H*-imidazol-4-yl)propenoic acid, **1**) has been first isolated by *Jaffe* from the urine of a peculiar dog in 1874 [1]. It is known as a deamination metabolite of histidine [2] that accumulates in the *stratum corneum* where it is a major UV-chromophore representing about 0.7% of the dry weight of the human skin [3]. Quite early it has been recognized that **1** could constitute a natural sunscreen since its UV-absorption spectrum ($\lambda_{max} = 275\,nm$) overlaps with the major erythmogenic region (290–310 nm) [4]. Upon irradiation with UV-light the naturally occuring (*E*)-**1** isomerizes partly to its diastereomer (*Z*)-**1**, which absorbs in this region as well [5]. In the 1980's *De Fabo et al.* demonstrated that (*Z*)-**1** is a mediator

* Corresponding author. E-mail: heinz.falk@jku.at

of UV-induced immunosuppression [6]. This immunosuppressive effect has also been linked to UV-induced skin cancer [7]. There are many investigations available in literature concerning the photodiastereomerization reaction of **1** [8]. Thus, *e.g.* the isomerization quantum yields at different wavelengths have been studied by *Morrison et al*. [9, 10], and more recently by *Hanson et al*. [5] and *Mohammad* [11]. In addition, the proportions of the diastereomers in the photostationary states have been demonstrated by *Laihia et al*. [12] to be dependent on *pH* values.

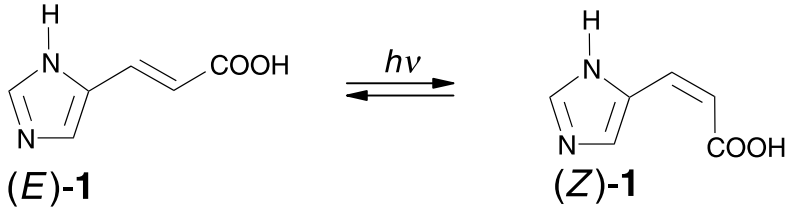

Such studies were exclusively focused upon free **1**. However, under physiological conditions a plethora of compounds including proteins will be present in addition to **1**. Pondering the constitution of **1**, one can imagine strong interactions or even complexation of **1** with constituents of such a matrix, and accordingly, the photodiastereomerization characteristics of free and associated **1** could be quite different. Given the physiological importance of the photodiastereomerization reaction we explored this topic in some detail and report the findings below.

Results and Discussions

Protic Equilibria of 1

Before setting out to investigate the photodiastereomerization of free and complexed **1** we decided to study the protonation–deprotonation equilibria of the diastereomers of **1** in some detail. This seemed to be important in peculiar, as it has been shown that

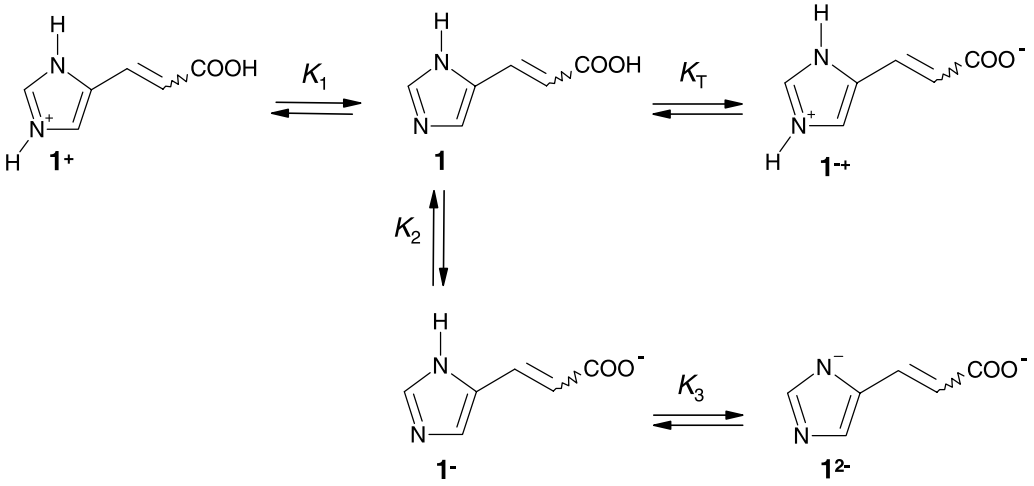

Fig. 1. Protonation states of **1**; the species possible in principle are the neutral (**1**), zwitterionic ($\mathbf{1}^{-+}$), protonated ($\mathbf{1}^{+}$), monodeprotonated ($\mathbf{1}^{-}$), and dideprotonated ($\mathbf{1}^{2-}$) forms

the photodiastereomerization reaction is dependent on *pH* [12] and wavelength [6]. Thus we constructed a quantitative picture of the various species present at different *pH* values by calculating the equilibrium concentrations of the different species of (*E*)- and (*Z*)-**1** as given in Fig. 1. Starting with the total concentration c_{Ua} of the pertinent diastereomer of **1** as given by $c_{Ua} = [\mathbf{1}^+] + [\mathbf{1}] + [\mathbf{1}^{+-}] + [\mathbf{1}^-] + [\mathbf{1}^{2-}]$ and deducing from Fig. 1 the relations $K_1 = [H^+][\mathbf{1}]/[\mathbf{1}^+]$, $K_2 = [H^+][\mathbf{1}^-]/[\mathbf{1}]$, $K_3 = [H^+][\mathbf{1}^{2-}]/[\mathbf{1}^-]$, and $K_T = [\mathbf{1}]/[\mathbf{1}^{+-}]$, the matrix equation system (1) could be derived. Using the *pK* values for (*E*)-**1** ($pK_1 = 4.85$ [13], $pK_2 = 4.67$ [13], $pK_T = 1.16$ [13], $pK_3 = 14.52$ was approximated by assigning to it the pK_a value of imidazole [14]) and (*Z*)-**1** ($pK_1 = 3.00$ [13], $pK_2 = 6.70$ [13], $pK_T = 1.25$ [13], and because there should be no significant difference between the two diastereomers in their imidazole NH deprotonation behaviour, $pK_3 = 14.52$) the different equilibrium concentrations of the species of (*E*)- and (*Z*)-**1** could then be calculated from (1) by means of Mathematica®.

$$\begin{pmatrix} 1 & 1 & 1 & 1 & 1 \\ -K_1 & [H^+] & 0 & 0 & 0 \\ 0 & -K_2 & 0 & [H^+] & 0 \\ 0 & 0 & 0 & -K_3 & [H^+] \\ 0 & 1 & -K_T & 0 & 0 \end{pmatrix} \cdot \begin{pmatrix} [\mathbf{1}^+] \\ [\mathbf{1}] \\ [\mathbf{1}^{-+}] \\ [\mathbf{1}^-] \\ [\mathbf{1}^{2-}] \end{pmatrix} = \begin{pmatrix} c_{Ua} \\ 0 \\ 0 \\ 0 \\ 0 \end{pmatrix} \qquad (1)$$

The results of these calculations are visualized in Fig. 2, and they demonstrate that under physiological conditions ($pH \approx 5$–7) up to four species will coexist. Their relative concentrations vary strongly with the *pH* values. In addition, these concentrations will strongly differ for the two diastereomers for a given *pH* value. Thus, *e.g.* at *pH* 6 we find for (*E*)-**1** equal amounts of zwitterion $\mathbf{1}^{-+}$ and mono-deprotonated species $\mathbf{1}^-$ (≈48% both) together with a rather small amount (≈2%) of the protonated species $\mathbf{1}^+$, whereas for (*Z*)-**1** the main species is the zwitterion $\mathbf{1}^{-+}$ (≈82%) and the mono-deprotonated form $\mathbf{1}^-$ and the protonated species $\mathbf{1}^+$ are present in about 13 and 5% only. Accordingly, a highly complex photodiastereomerization behavior with respect to *pH* and irradiation wavelength could be envisaged because a series of different species with different photochemical properties will be present in strongly varying relative concentrations depending on the *pH* of the solution. Of course, additional complications could arise from a variety of rotamers and tautomers possible for the individual prototropic species.

Although there have been several studies of ^{1}H NMR spectra of the diastereomers of **1** (*e.g.* Ref. [15]) no consistently assigned set of signals was available for aqueous solutions. Thus, to acquire a reliable *in situ* analytical tool to investigate quantitative aspects of photodiastereomerization such a set (Fig. 3) was derived by 2D methods. By tracing the various shifts of these signals in dependence of *pH* a direct tool to assess the photodiastereomerization was established. Because it turned out that direct observation of the photodiastereomerization of complexed systems was not possible due to the low concentrations of **1** used, and moreover, to severe signal overlaps, we used the ^{1}H NMR data to calibrate the UV spectroscopic method.

*Photodiastereomerization of **1***

The first problem to solve was to determine whether there is indeed complexation between the diastereomers of **1** and human serum albumin (*HSA*), which we chose

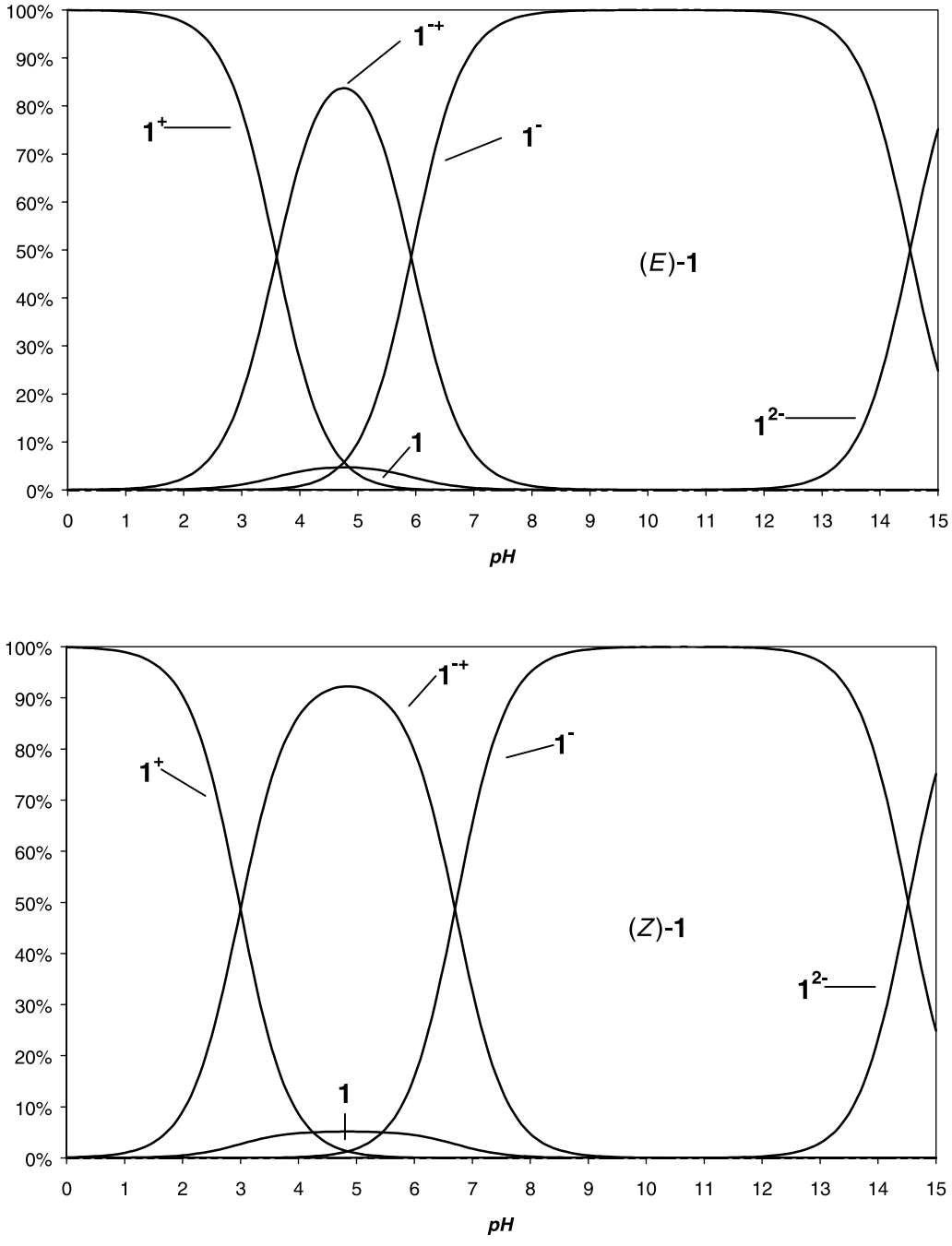

Fig. 2. Calculated *pH*-dependence of the concentrations of the protic species of (*E*)- and (*Z*)-urocanic acid (**1**): the neutral **1**, the zwitterion $\mathbf{1}^{-+}$, the protonated $\mathbf{1}^{+}$, the monodeprotonated $\mathbf{1}^{-}$, and the dideprotonated $\mathbf{1}^{2-}$

as a simple protein model for the complex matrix of the skin. To estimate the complex binding properties the protein fluorescence decrease ($\lambda_{EX} = 280\,nm$, $\lambda_{EM} = 340\,nm$) induced by ligand binding was used [16]. Accordingly, the

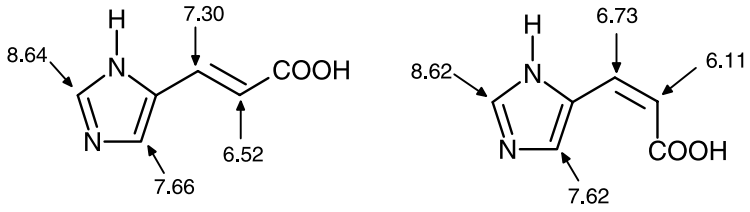

Fig. 3. Assignment of the ^{1}H NMR shifts of (*Z*)- and (*E*)-**1** in aqueous (D_2O) solution, $pH = 5.0$

fluorescence of *HSA* was measured in the presence and absence of ligand at various concentrations of (*E*)-**1** (0–$4.8 \cdot 10^{-4}$ mol·dm^{-3}) in aqueous solutions ($pH = 7.0$) at a protein concentration of $3.9 \cdot 10^{-6}$ mol·dm^{-3}. The binding constant K_b of (*E*)-**1** to *HSA* was then calculated from a *Scatchard* linearization [17]: $[B]/[F] = K_b \cdot [R_T] - K_b \cdot [B]$, where $[B]$ and $[F]$ are the bound and the free ligand concentrations and $[R_T]$ is the total receptor (*HSA*) concentration. The plot displayed in Fig. 4 led to a binding constant $K_b = 4.1 \cdot 10^4$ mol·dm^{-3}. Although this value was derived for the (*E*)-diastereomer we infer that both diastereomers of **1** will be bound similarly tightly to *HSA*.

Irradiation of free aqueous (*E*)-**1** and a solution of its complex with *HSA* ($c_1 = 3.7 \cdot 10^{-5}$ mol·dm^{-3} and a ratio (*E*)-**1** to *HSA* of 50:1 in water, $pH = 7.0$) resulted in a decrease of the UV absorbances because of the lower extinction

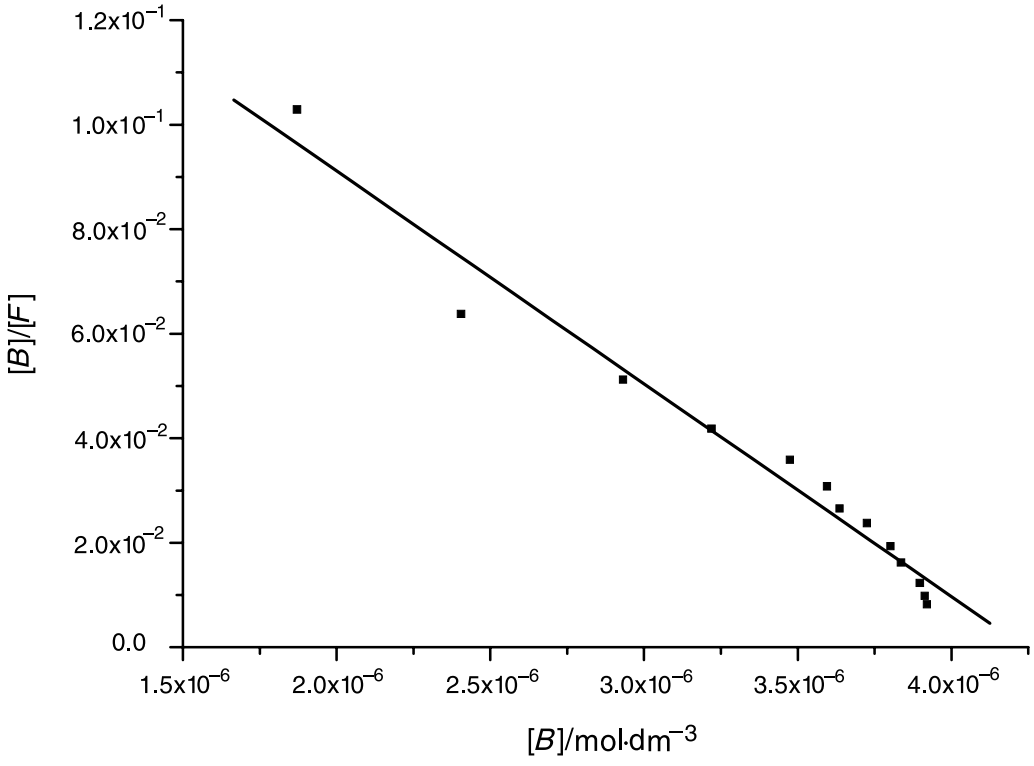

Fig. 4. *Scatchard* plot for the complexation of (*E*)-**1** with *HSA*

coefficient of the resulting (*Z*)-diastereomer. NMR detection for estimating the ratio of the diastereomers was not possible due to the low concentration used in these experiments. However, it was used to assess absolute concentrations of the diastereomers for concentrated solutions and to derive the corresponding relative absorptions upon dilution. Because the ε value for (*E*)-**1** was found to be non-linear for the concentration region used, the logarithmic adjustment $\varepsilon = 17750 + 1022.3 \cdot e^{-x/1.1188}$ was applied, where x is the molar concentration. The measured absorbance is the sum of the absorbance of the two diastereomers: $E = E_E + E_Z = \varepsilon_E \cdot c_E \cdot d + \varepsilon_Z \cdot c_Z \cdot d$, where d is 1 cm and the sum of c_E and c_Z is $3.7 \cdot 10^{-5}$ mol·dm^{-3} (the initial concentration of (*E*)-**1**). By means of these relationships the concentrations of (*E*)- and (*Z*)-**1** during and after irradiation when reaching the photostationary equilibrium could be derived. Although the photodiastereomerization rates did not differ significantly, the observed ratio of the two diastereomers in the free state was found to differ significantly amounting to 33:67 for the aqueous solution, but to 50:50 for the *HSA*-complexed state. This difference does not derive from the one observed for solutions of different *pH* values [12] because the *pH* values of the free and complexed system were kept at 7.0. Obviously, the differential stabilization of the orthogonal state(s) [12] leading to the observed photodiastereomer ratio is strongly dependent on the complexation of the diastereomeric states. This result documents clearly that the influence of the matrix in the physiological system is not negligible as has been inferred recently [12], and has to be taken into account in investigations of the photochemical behavior of **1**. Interestingly enough, the photoequilibrium ratio of (*Z*)-**1**:(*E*)-**1** in sun-exposed skin has been found to amount to 50:50 [7]. Thus the complexation of **1** by skin constituents is modeled perfectly by its complexation by *HSA*.

Thermal Diastereomerization Reaction

Because of the importance of the photodiastereomerization reaction the question of a possible thermal isomerization accompanying the photoreaction is highly interesting and has not yet been addressed explicitly to our knowledge. To evaluate this possible influence, we thermally equilibrated samples of various mixtures of (*E*)- and (*Z*)-**1** dissolved in D_2O. The concentrations of the diastereomers were followed by ^{1}H NMR spectroscopy of the temperated samples. The first mixture investigated consisted of 67% (*Z*)-**1** and 33% (*E*)-**1** (the photostationary state concentrations), the other one contained 15% (*Z*)-**1** and 85% (*E*)-**1** (which is far away from the photostationary equilibrium). After thermal equilibration for 32 h at 80°C samples were withdrawn and the temperature was set to 90°C for additional 14 h. No significant concentration changes could be detected in all samples. From this observation we extrapolated a lower limit for the *Arrhenius* activation energy of $>250\,\text{kJ}\cdot\text{mol}^{-1}$. Thus the kinetic stabilities of the diastereomers of **1** were found to be quite extraordinarily high. Accordingly, it can be concluded that the (*Z*)-diastereomer of urocanic acid ((*Z*)-**1**) found in the human skin [8] cannot originate from a thermal equilibration, but is exclusively due to photodiastereomerization. In addition, a disturbance of photodiastereomerization experiments by a thermal back-reaction of the (*E*)-diasteromer can thus be ruled out. The latter reaction could have been envisaged from the thermodynamic instability of the (*E*)-diastereomer,

which we estimated by AM1 calculations to amount to about $9\,kJ\cdot mol^{-1}$ ($\Delta H_f = -115\,kJ\cdot mol^{-1}$ for the (*E*)-**1** and $-124\,kJ\cdot mol^{-1}$ for the (*Z*)-**1** diastereomer – *cf.* Ref. [18]).

Epilogue: Light-Induced pH-Jump

As discussed in the first chapter (see Fig. 2), the diastereomers of **1** display different and sensitive prototropic behaviors with respect to the *pH* values within the physiological *pH* region. This triggered the idea that the photodiastereomerization reaction could be used to initiate a photoinduced persistent *pH* jump derived from the photoinduced shift of the proportion of the two diastereomers at a given *pH* value. Indeed, when aqueous solutions of (*E*)-**1** ($c = 1\cdot10^{-3}$ $mol\cdot dm^{-3}$) with different starting *pH* values were irradiated with UV-light under stirring and concomitant *pH*-measurement the *pH* values changed. Thus, *e.g.* when starting at *pH* 3.48, the solution equilibrated upon irradiation at *pH* 3.36, and when starting at *pH* 8.32, *pH* 8.46 was attained. Of course, by exchanging the (*E*)-diastereomer by the (*Z*) configured one a *pH* jump in the opposite direction will be obtained. Since photodiastereomerizations are very fast reactions (ps to ns), this behavior opens the possibility to achieve laser induced ultrafast *pH* jumps yielding acidification or basification of solutions of pertinent biomolecules, like proteins or polynucleotides. Such jumps using, as proposed, one of the diastereomers of urocanic acid (**1**) will be ultrafast (diffusion controlled), persistent, and bidirectional depending on which diastereomer is initially used at a certain *pH* value. Compared with this new methodology the conventional techniques are rather limited. Thus, commonly *pH* jumps are induced by means of stopped-flow experiments [19] in the slow reaction domain and by means of the photodissociation of *o*-nitrobenzaldehyde in the fast reaction area [20]. Although the latter method yields persistent jumps it is unidirectional allowing for acidification of a system only.

Experimental

(*E*)-Urocanic acid ((*E*)-**1**) and *HSA* ($M = 66439$) were of commercial origin (Sigma). Photodiastereomerizations of the stirred samples were executed by means of a Hanau TQ 150 Z1 UV-lamp in SiO_2 cells under Ar atmosphere in aqueous solution (dist. H_2O, D_2O). (*Z*)-Urocanic acid ((*Z*)-**1**) was isolated from such photodiastereomerization batches by means of preparative HPLC (Dionex: P 608 pump, ASI-100 automated sample injector, PDA detector, LiChrosorb RP 18 (7 μm) column, $d = 10$ mm, $l = 250$ mm, distilled H_2O). ^1H NMR spectra were recorded by means of a Bruker Avance 200 MHz, 2D correlation experiments (COSY) were set up using the commercially available tools. The UV and fluorescence spectra were obtained on the Varian Cary 100 Bio and Hitachi F-4010 spectrometer using SiO_2 cells, $d = 1$ cm. Thermal isomerizations were conducted using a mgw Lauda Thermo-Boy and *pH* measurements were done by means of a Orion Model 290 A with a Hamilton Slimtrode or Hamilton Slintrode (directly inserted into the NMR tube). Calculations were executed using Mathematica®.

Acknowledgment

We are grateful to *M. Kitzmüller* for assistance in the mathematical calculations.

References

[1] Jaffe M (1874) Ber dtsch chem Ges **7**: 1669
[2] Baden HP, Pathak MA, Butler D (1966) Nature **210**: 732; Baden HP, Pathak MA (1967) J Invest Derm **48**: 11
[3] Tabachnick J (1957) Arch Biochem Biophys **70**: 295
[4] Zenisek A, Kral J, Hais I (1955) Biochim Biophys Acta **18**: 589
[5] Hanson KM, Li B, Simon JD (1997) J Am Chem Soc **119**: 2715
[6] De Fabo EC, Noonan FP (1983) J Exp Med **158**: 84
[7] Norval M (2001) J Photochem Photobiol **B63**: 28
[8] for reviews see: Mohammad T, Morrison H, HogenEsch H (1999) Photochem Photobiol **69**: 115; Simon JD (2000) Acc Chem Res **33**: 307
[9] Morrison H, Bernasconi C, Pandey G (1984) Photochem Photobiol **40**: 549
[10] Morrsion H, Avnir D, Bernasconi C, Fagan G (1980) Photochem Photobiol **32**: 711
[11] Mohammad T (2002) Tetrahedron Lett **43**: 8897
[12] Laihia JK, Lemmetyinen H, Pasanen P, Jansen CT (1996) J Photochem Photobiol B **33**: 211
[13] Halle JC, Pichon C, Terrier F (1984) J Biol Chem **259**: 4142
[14] Barton D, Ollis D (eds) (1979) Comprehensive Organic Chemistry. In: Sammes PG (ed) Heterocyclic Compounds, vol 4. Pergamon Press
[15] Neuvonen H, Neuvonen K (1998) J Chem Soc Perkin Trans 2, 1665
[16] Sulkowska A, Bojko B, Rownicka J, Pentak D, Sulkowski W (2003) J Mol Struct **651–653**: 237
[17] Hiratsuka T (1990) J Biol Chem **265**: 18786
[18] Lahti A, Hotokka M, Neuvonen K, Äyräs P (1995) J Mol Struct Theochem **331**: 169
[19] e.g.: Nagel JHA, Gultyaev AP, Öistämö KJ, Gerdes K, Pleij CWA (2002) Nucl Acids Res **30**: 63
[20] Viappiani C, Bonetti G, Carcelli M, Ferrari F, Sternieri A (1998) Rev Sci Instrum **69**: 270; Abbruzzetti S, Crema E, Masino L, Vecli A, Viappiani C, Small JR, Libertini LJ, Small E (2000) Biophys J **78**: 405; Choi J, Hirota N, Terazima M (2001) J Phys Chem **105**: 12